

CREEP LIFE PREDICTIONS FOR STRUCTURES SUBJECT TO VARIABLE LOADING

R. A. AINSWORTH and I. W. GOODALL

Central Electricity Generating Board, Berkeley Nuclear Laboratories, Berkeley, Gloucestershire, England

(Received 1 July 1975; revised 18 December 1975)

Abstract—Previous work which established upper and lower bounds on the creep life of steadily loaded structures is extended to cater for load and temperature variations in non-homogeneous structures. The investigation is limited to the range where short term plasticity and fatigue damage can be ignored. For proportional loading, the upper bound which is based on limit analysis, is similar in form to that for constant loading. In the more general case, the upper bound is less stringent and is based on the mean load and temperature distribution over the lifetime. A lower bound on life is taken as the time for the first part of the structure to fail.

The bounds are applied to three simple structures. For proportional loading the upper bound predicts the lifetime with the same accuracy as for constant loading except for extreme load variations. The presence of a temperature distribution alters the accuracy of the upper bound prediction but in most cases the change is small. In contrast, the lower bound is very sensitive to the temperature gradient.

The authors use these results to develop approximate techniques for estimating the creep life of components subjected to variable loads and temperature distributions. Simplified design procedures based on the upper bound are examined and suitable amendments are proposed.

NOTATION

α	scalar multiplier
α_0	radius ratio $\{= a/b\}$
β_0	radius ratio $\{= r_i/r_0\}$
δ_{ij}	Kronecker's delta
$\dot{\epsilon}_{ij}$	strain-rate tensor
θ	temperature
λ, μ	parameters describing loading cycle
σ_e	equivalent stress $\{= (\frac{1}{2} S_{ij} S_{ij})^{1/2}\}$
$\sigma_r, \sigma_\theta, \sigma_z$	radial, hoop and axial stress components, respectively
σ_{ij}	stress tensor
$\phi(\sigma_{ij})$	creep energy dissipation surface
χ	ratio of collapse load to load for first yield
$\psi(\sigma_{ij})$	rupture surface
a, b	internal and external radii of disc
\dot{D}	creep damage rate
$g(\theta)$	positive function of temperature
m	rupture index
n	creep deformation index
p	pressure
P_i	applied loads
r	radius
r_i, r_0	internal and external radii of tube
S	surface
S_{ij}	deviatoric stress tensor $\{= \sigma_{ij} - \frac{1}{3} \delta_{ij} \sigma_{kk}\}$
t	time
t_r	rupture time
t^*	upper bound rupture time
t_f	time of failure of first part of structure
T	period of cycle
\dot{u}_i	displacement rates
\dot{v}_{ij}	creep strain rates
V	volume
x	spatial co-ordinates

1. INTRODUCTION

The paper considers structures subjected to load and temperature variations within the range where short term plasticity and fatigue damage can be ignored. Under such conditions, structures operating at high temperature will fail ultimately by creep rupture mechanisms. Initial rupture occurs in the region of stress concentration but the life of the structure is not exhausted until sufficient material has failed for a collapse mechanism to be formed. This presumes the material

is ductile so that it can tolerate large amounts of tertiary deformation without cracking. This assumption is made throughout the paper.

The initial failure of a structure may be predicted from a knowledge of the stationary creep stress distribution. However, this initial or lower bound failure time is very pessimistic when the material is ductile or when high stress concentrations are present[1]. A complete solution requires the analysis of failure propagation from initial failure to ultimate collapse. By assuming idealised creep laws, a number of authors (Kachanov[2], Hayhurst[3], Hayhurst and Leckie[4]) have analysed the propagation of failure for some simple structures. For more complex structures, Goodall *et al.*[5] have obtained solutions using finite element methods. However, such methods require large amounts of computer time and are unlikely to become part of the normal design process.

For structures subjected to steady loading, Goodall and Cockcroft[1] have obtained an upper bound on the rupture life. This bound is based on limit analysis and lies close to the true rupture life for many simple structures. Because the upper bound is unconservative, detailed experimental and theoretical study is required to develop correction factors which may be used with the upper bound to give a safe result. Developing this approach, Goodall *et al.*[5] have shown that it is possible to predict the life of structures from a knowledge of the rupture stress of the material, the limit load and the elastic stress concentration factor.

An alternative approach has been presented by Martin and Leckie[6] and by Leckie and Hayhurst[7] who have derived lower bound failure times for kinematically determinate structures. For high values of the creep deformation index and for materials with creep deformation and rupture surfaces of the same form, this lower bound result can be expressed in terms of the limit load[7]. The result obtained is identical to the upper bound result of Goodall and Cockcroft[1] and hence both methods should be exact under such circumstances. This is reflected in the excellent agreement between experimental and predicted behaviour obtained by Leckie and Hayhurst[7]. For a material (copper) with deformation and rupture surfaces of different form, the experimental results[7] appear to agree well with both the lower bound[7] and the upper bound[1].

In the present paper, the upper bound of Goodall and Cockcroft[1] is extended to cover time-varying loading conditions and time-dependent spatially varying temperature distributions. The previous result for constant loading[1] is obtained as a special case. The effects of load variations and temperature distributions are examined by studying three simple structures. The simplified approach to life assessment proposed by Goodall *et al.*[5] is examined for these structures and a suitable extension is proposed.

2. BASIC ASSUMPTIONS AND DESCRIPTION OF MATERIAL BEHAVIOUR

Consider a body of volume, V , surface, S , with negligible body forces. This is subject to a given history of loading $P_i(t)$ over part S_p of S and to zero surface velocities over the remainder S_u . The temperature distribution $\theta(\mathbf{x}, t)$ is a given function of position, \mathbf{x} , and time, t . The virtual work equation is

$$\int_v \sigma_{ij} \dot{\epsilon}_{ij} dV = \int_{S_p} P_i \dot{U}_i dS \quad (2.1)$$

where σ_{ij} is any stress distribution in equilibrium with the applied loads P_i and $\dot{\epsilon}_{ij}$ is any kinematically admissible strain-rate field with corresponding velocities \dot{U}_i . All deformations are assumed small so that changes in geometry may be neglected.

It is assumed that creep rupture under a varying stress and temperature history is governed by the life fraction rule of Robinson[8]. Consequently, for a uniaxial stress history, $\sigma(t)$, and a temperature history, $\theta(t)$, rupture occurs at a time t_r given by

$$\int_0^{t_r} \frac{dt}{t_r(\sigma, \theta)} = 1 \quad (2.2)$$

where $t_r(\sigma, \theta)$ is the rupture time corresponding to a constant stress level, σ , and a constant temperature, θ . For uniaxial failure in the stress range of practical interest, it is usually

sufficiently accurate to assume that

$$g(\theta)\sigma^m t_r(\sigma, \theta) = \text{constant.}$$

For multiaxial stress conditions it is assumed that the rate of creep damage, D , at any point is given by

$$\dot{D} = \psi(\sigma_{ij})g(\theta) \quad (2.3)$$

where $\psi(\sigma_{ij})$ is a positive, homogeneous function of degree m in σ_{ij} , and $g(\theta)$ is a positive function of the temperature, θ . $\psi(\sigma_{ij})$ is assumed to be convex, so that any two stresses, $\sigma_{ij}^A, \sigma_{ij}^B$, satisfy the inequality of Hill[9],

$$\psi(\sigma_{ij}^A) - \psi(\sigma_{ij}^B) - (\sigma_{ij}^A - \sigma_{ij}^B) \frac{\partial \psi(\sigma_{ij}^B)}{\partial \sigma_{ij}^B} \geq 0. \quad (2.4)$$

The creep resistance of the material is taken to be exhausted when the accumulated damage is arbitrarily unity. If the lifetime of the structure is t_r , then from eqn (2.3)

$$\int_0^{t_r} \psi(\sigma_{ij})g(\theta) dt \leq 1 \quad \text{everywhere.} \quad (2.5)$$

At failure the equality holds at sufficient places for collapse to occur. Equation (2.5) reduces to eqn (2.2) for uniaxial conditions.

3. THE UPPER BOUND

(a) *For proportional loading and time independent temperature distributions*

Consider a structure subjected to an applied loading system, $P_i(t)$, which varies in a proportional manner with time. Consequently

$$P_i(t) = P_i^0 \mu(t) \quad (3.1)$$

where $\mu(t)$ is a time dependent scalar quantity and P_i^0 is the loading at some arbitrary time t_0 . Furthermore, it is assumed that the temperature varies in space but not with time. At any instant, t , there is a stress distribution, σ_{ij}^* , in equilibrium with the applied loads, $P_i(t)$, which minimises the maximum value of $\psi(\sigma_{ij})g(\theta)$ within the structure. Denoting this maximum value by $t^*(t)^{-1}$,

$$\text{Min}_{\sigma_{ij}} \text{Max}_{\mathbf{x}} \psi(\sigma_{ij})g(\theta) = \frac{1}{t^*(t)}. \quad (3.2)$$

Solution of this extremum problem is analogous to the determination of the limit load of a structure composed of material with a yield criterion $\psi(\sigma_{ij})g(\theta) \leq (t^*)^{-1}$. Consequently the stress distribution σ_{ij}^* determines a collapse mechanism with an associated kinematically admissible strain distribution, normal to the yield surface, given by (see, for example, Hill[10]),

$$\epsilon_{ij}^* = Kg(\theta)f(t) \frac{\partial \psi(\sigma_{ij}^*)}{\partial \sigma_{ij}^*} \quad (3.3)$$

where

$$\left. \begin{aligned} K = 0 & \quad \text{for } \psi(\sigma_{ij}^*)g(\theta) < \frac{1}{t^*} \\ K \geq 0 & \quad \text{for } \psi(\sigma_{ij}^*)g(\theta) = \frac{1}{t^*} \end{aligned} \right\} \quad (3.4)$$

Here K is a scalar quantity which varies with position \mathbf{x} but is defined to be independent of time by absorbing the time dependence into $f(t)$. This is admissible in view of eqn (3.1).

Applying inequality (2.4) to the actual stress distribution σ_{ij} and the limit stress distribution σ_{ij}^* and multiplying by $Kg(\theta)$ gives

$$K\psi(\sigma_{ij})g(\theta) \geq K\psi(\sigma_{ij}^*)g(\theta) + K \frac{\partial\psi(\sigma_{ij}^*)}{\partial\sigma_{ij}^*} g(\theta)(\sigma_{ij} - \sigma_{ij}^*).$$

Integrating over the lifetime noting relations (3.3), (3.4), and (2.5),

$$K \geq K \int_0^{t_r} \frac{dt}{t^*(t)} + \int_0^{t_r} \frac{\epsilon_{ij}^*}{f(t)} (\sigma_{ij} - \sigma_{ij}^*) dt. \quad (3.5)$$

Integrating (3.5) over the volume using the virtual work expression (2.1),

$$\left\{ 1 - \int_0^{t_r} \frac{dt}{t^*(t)} \right\} \int_0 K dV \geq 0.$$

Since K is non-negative from the principle of maximum plastic work [10],

$$\int_0^{t_r} \frac{dt}{t^*(t)} \leq 1. \quad (3.6)$$

This result may be expressed in a slightly different, and perhaps more meaningful form. Using eqn (3.1), $t^*(t) = t_0^* \mu^{-m}(t)$ where t_0^* is the upper bound failure time determined for the constant loading P_i^0 . Thus equation (3.6) becomes,

$$\int_0^{t_r} \mu^m(t) dt \leq t_0^*. \quad (3.7)$$

This implies that the cumulative damage law that applies to the stresses in a uniaxial test may also be applied to the load factor $\mu(t)$ occurring during proportional loading. In addition, it may be seen that for constant loads and temperature distributions, inequality (3.6) reduces simply to,

$$t_r \leq t^* \quad (3.8)$$

which is the result obtained by Goodall and Cockcroft [1] for steady loading.

(b) Arbitrary load and temperature variations

For more general loading, the scalar K is time-dependent and inequality (3.6) is not valid. However, an upper bound may be obtained by using the limit solution $\bar{\sigma}_{ij}^*$, \bar{t}^* derived for the mean load \bar{P}_i and a mean temperature effect $\bar{g}(\theta)$ defined by

$$\left. \begin{aligned} \bar{P}_i &= \frac{1}{t_r} \int_0^{t_r} P_i dt \\ \bar{g}(\theta) &= \left[\frac{1}{t_r} \int_0^{t_r} g(\theta)^{-1/(m-1)} dt \right]^{-(m-1)}. \end{aligned} \right\} \quad (3.9)$$

Then relations (3.3) and (3.4) are replaced by

$$\bar{\epsilon}_{ij}^* = \bar{K} \frac{\partial\psi(\bar{\sigma}_{ij}^*)}{\partial\bar{\sigma}_{ij}^*} \bar{g}(\theta) \quad (3.10)$$

where

$$\left. \begin{aligned} \bar{K} &= 0 \quad \text{for } \psi(\bar{\sigma}_{ij}^*)\bar{g}(\theta) < (\bar{t}^*)^{-1} \\ \bar{K} &\geq 0 \quad \text{for } \psi(\bar{\sigma}_{ij}^*)\bar{g}(\theta) = (\bar{t}^*)^{-1}. \end{aligned} \right\} \quad (3.11)$$

Applying inequality (2.4) for the actual stress σ_{ij} and for the stress, $\alpha\bar{\sigma}_{ij}^*$ where α is a

time-dependent, positive scalar,

$$\psi(\sigma_{ij}) - \psi(\alpha \bar{\sigma}_{ij}^*) - \frac{\partial \psi(\alpha \bar{\sigma}_{ij}^*)}{\alpha \partial \bar{\sigma}_{ij}^*} (\sigma_{ij} - \alpha \bar{\sigma}_{ij}^*) \geq 0. \quad (3.12)$$

Multiplying eqn (3.12) by $\bar{K}g(\theta)$ and using the homogeneity of $\psi(\sigma_{ij})$ and eqns (3.10), (3.11),

$$\bar{K}\psi(\sigma_{ij})g(\theta) - \frac{\bar{K}\alpha^m g(\theta)}{\bar{g}(\theta)\bar{t}^*} - \frac{\alpha^{m-1}g(\theta)}{\bar{g}(\theta)} \bar{\epsilon}_{ij}^* (\sigma_{ij} - \alpha \bar{\sigma}_{ij}^*) \geq 0. \quad (3.13)$$

The scalar, α , is chosen so that $\alpha^{m-1}g(\theta) = \bar{g}(\theta)$. In view of eqn (3.9), the scalar α has a mean value of unity over the lifetime. Integrating eqn (3.13) over the lifetime and then over the volume, noting eqn (2.5), and the virtual work eqn (2.1), gives

$$t_r \leq \bar{t}^*. \quad (3.14)$$

It should be noted that eqn (3.14) is identical to eqn (3.8) for constant loading conditions, but for proportional loading it can readily be shown to be a less stringent upper bound.

In the derivation of inequalities (3.6) and (3.14), $g(\theta)$ has been presented as a temperature effect. However, the results are clearly unaffected if $g(\theta)$ describes the spatial variation of rupture properties caused by other effects. For instance, the structure could be initially non-homogeneous due to the presence of welds or the effects of heat treatment.

4. THE LOWER BOUND

The upper bounds presented in Section 3 are determined purely by the creep rupture behaviour. However, to obtain a lower bound, information about the creep deformation behaviour is also required. For materials which exhibit a prolonged period of secondary creep, a lower bound under constant loading can be taken as the rupture life corresponding to the maximum stress occurring in the stationary state[1]. This method will be acceptable if the redistribution time to the stationary state is small compared to the lifetime and if the peak stress is sufficiently low for a prolonged period of secondary creep to be present. A rapid method of estimating redistribution times has been given by Calladine[11]. For practical purposes, the assumptions are reasonable since structures designed for lifetimes in excess of twenty years must have low operating stresses.

Under cyclic loading, a structure settles down to exhibit a periodic response when it may be termed to be in a cyclic stationary state. For cycle times which are short compared to the lifetime, a good approximation to the cyclic stationary state may be obtained by neglecting the effects of stress redistribution within the cycle. Ainsworth[12] has shown that such a solution may be obtained using methods analogous to those used to determine the constant load stationary solution. The lower bound is then taken as the time to failure at the point in the structure which has the maximum damage per cycle. Denoting the steady cyclic stress distribution by σ_{ij}^{sc} for a cycle time T ,

$$t_r \geq \frac{1}{\text{Max}_v \left\{ \frac{1}{T} \int_0^T \psi(\sigma_{ij}^{sc})g(\theta) dt \right\}}. \quad (4.1)$$

This bound is only acceptable if the redistribution time to the cyclic stationary state is small compared to the lifetime and if the stresses are sufficiently low for a prolonged period of secondary creep to be present. This latter requirement may also be considered as the requirement that damage has no effect on the creep rates until times close to the failure time. As in the case of constant loading, the assumptions should be reasonable for practical structures.

For steady loading, a rapid method of evaluating the maximum stress, and hence the lower bound, has been presented by Calladine[13]. However, from a practical viewpoint, it is worth noting that the lower bound is, in general, more difficult to evaluate than the upper bound.

5. APPLICATION TO SIMPLE STRUCTURES

In order to determine whether a simple design approach can be developed for structures subjected to time-dependent loading, it is necessary to examine some typical structures. In this section, three geometries are examined: a two-bar mechanism, a thin circular disc and a pipe. For the simple structures considered, the rupture and deformation surfaces are assumed to be

$$\psi(\sigma_{ij}) = \sigma_e^m, \quad \phi(\sigma_{ij}) = \sigma_e^{n+1} \quad (5.1)$$

where σ_e is the von Mises equivalent stress. Creep strains, normal to the deformation surface, are then given by

$$\dot{v}_{ij} = \frac{3}{2} \sigma_e^{n-1} S_{ij} g(\theta) \quad (5.2)$$

where S_{ij} is the deviatoric stress tensor. For all cases, the structure is assumed to be in the stationary (or cyclic stationary) state until initial failure and subsequently to be in a succession of stationary states with failed material only able to withstand a hydrostatic stress.

(a) *Two-bar structure*

The structure shown in Fig. 1 is considered. It consists of two bars with areas A_1 , A_2 and lengths l_1 , l_2 . The arrangement is constrained to move vertically and is loaded with a vertical force, P , which varies as shown in Fig. 2. By neglecting the effects of stress redistribution within the cycle, it is possible to obtain the steady cyclic solution and to compare the upper and lower bounds with the "exact" solution. For a given lifetime, the load bearing capacities P^u , P , P^L for the upper bound, "exact" and lower bound solutions respectively, are compared in Fig. 3. Since the loading is proportional, the upper bound solution given by eqn (3.7) is used. It may be seen that the errors in both bounds are increased over the steady load values ($\lambda = 1$ or $\mu = 1$), but the increases are only significant when the load change is large *and* the larger load acts for a small fraction of the total time.

(b) *Thin circular disc*

Another case of proportional loading is the disc shown in Fig. 4 subjected to a radial tension which varies as shown in Fig. 2. The stationary solution is obtained by a rapidly convergent

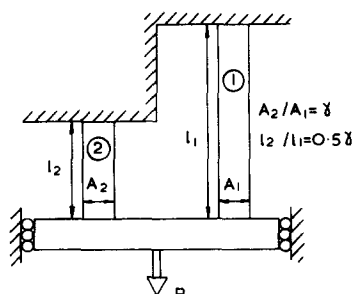


Fig. 1. Geometry of two-bar structure.

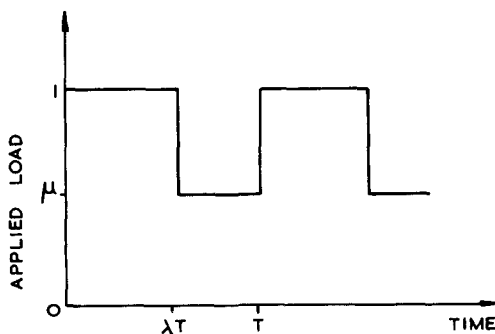


Fig. 2. Load variation.

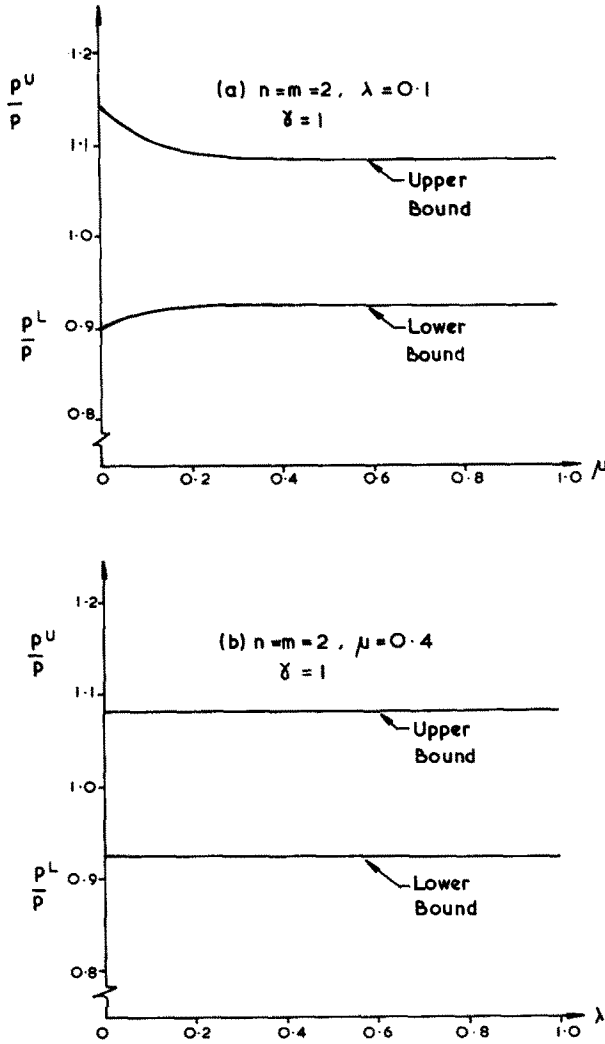


Fig. 3. Two-bar, comparison of bounds.

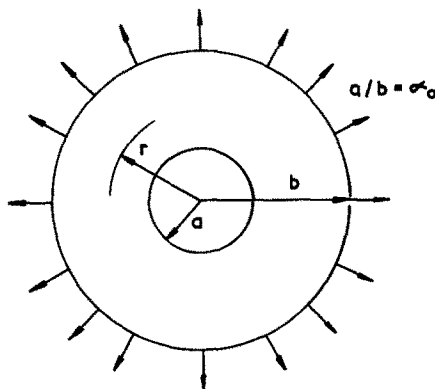


Fig. 4. Geometry of disc.

iterative method described by Rabotnov [14] for steady loading and extended to cyclic loading by Ainsworth [12]. Initial failure occurs at the inside and propagates rapidly through the disc (see Fig. 5). By evaluating a succession of steady cyclic solutions, the actual failure time of the disc is obtained.

For the creep index, $n = 1$ and rupture index, $m = 2$, it is possible to obtain an analytic solution for the final rupture time (Appendix 1). This enables the numerical procedure to be checked and indicates that the numerical results are accurate to within 1%. The upper bound given by eqn (3.7) can be obtained analytically and the derivation is given in Appendix 2. For a

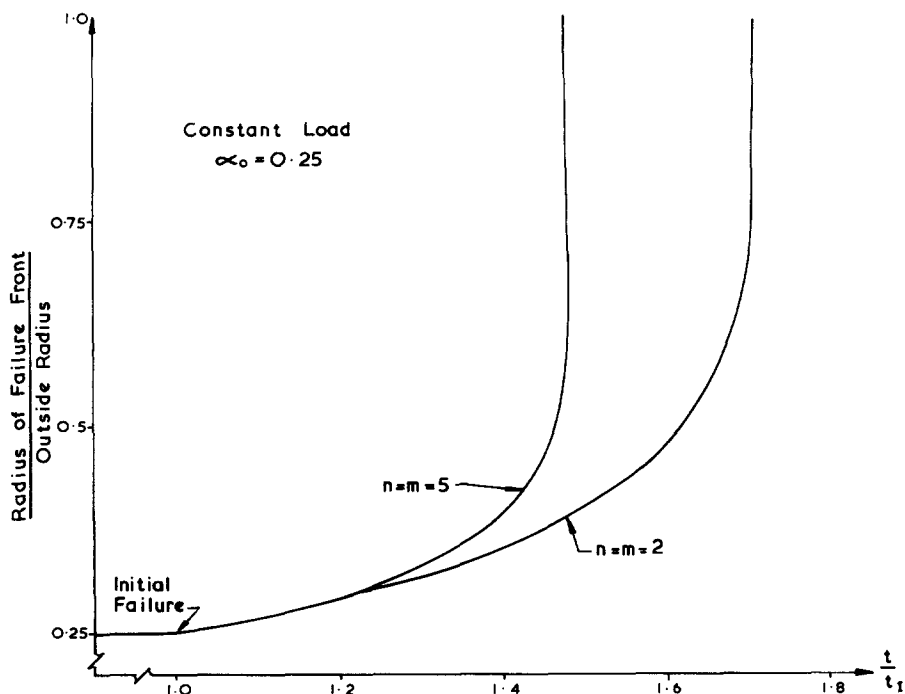


Fig. 5. Disc, propagation of failure front.

given lifetime of the structure, the load bearing capacities are compared in Fig. 6. As in the case of the two-bar structure, the errors in the bounds only differ significantly from the steady load errors when the load change is large *and* the larger load acts for small fraction of the total time.

(c) *Tube under internal pressure*

This structure is analysed in order to assess the effect of temperature distributions on the accuracy of the bounds. The geometry of the tube is shown in Fig. 7. It is subjected to a constant internal pressure and to a radial temperature distribution caused by maintaining the inner and outer surfaces at differing temperatures θ_i and θ_o . Plane strain conditions are assumed. Detailed analysis of the structure is given in Appendix 3. The temperature effect $g(\theta)$ is taken to be of the form

$$g(\theta) = \exp \{ \alpha (\theta - \theta_i) \}.$$

In order to give a quantitative value to the temperature difference, for the results plotted, α has been taken as $4.4 \times 10^{-2}/\text{deg.}$ (Blackburn[15] for ASTM 304 and 316 stainless steels at 600°C).

The failure front may propagate from the inside or the outside or failure may occur at all radii simultaneously. In the last case, the upper and lower bounds coincide and are, therefore, exact. Some typical results are presented in Figs. 8–10 for the upper bound, exact, and lower bound pressures p^u , p , p^L to cause failure in a given time. For the case $n = m = 2$ the upper bound depends only on the absolute value of $(\theta_o - \theta_i)$. In general, however, the bounds depend on which surface is at the higher temperature (see Fig. 10). It may be seen from Fig. 10 that the ratio (p^u/p) is much less sensitive to the temperature difference and the indices m, n than the lower bound ratio (p^L/p) . Also the bounds improve as the radius ratio β_o increases which is to be expected, for when the tubes are thin they become statically determinate.

6. CONCLUDING REMARKS

Bounds on the life of structures subjected to variable loading have been derived. In general, the upper bound, based on limit analysis, depends on the mean load and a mean temperature distribution. For the case of proportional loading, the upper bound is identical in form to the bound for constant loading. A lower bound on life is taken as the time when the first part of the structure fails. Although the bounds derived are valid for materials which may have different

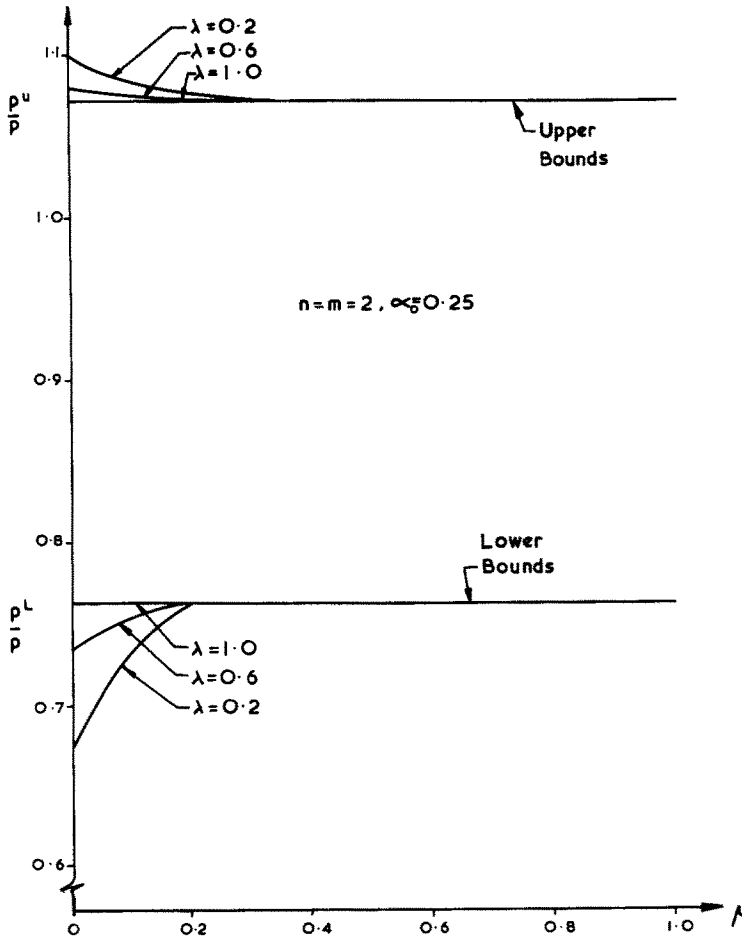


Fig. 6. Disc, comparison of bounds.

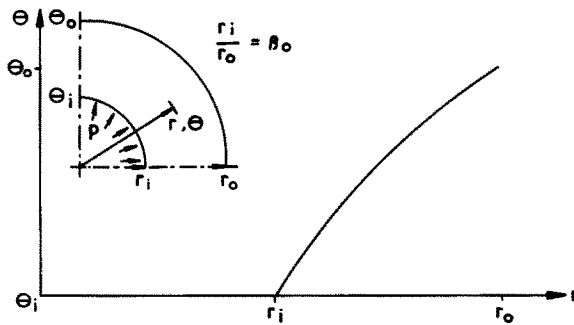


Fig. 7. Geometry and temperature distribution of tube.

rupture and deformation surfaces, the errors in the bounds will clearly depend on whether or not the surfaces are similar. In this section, attention is restricted to materials which have similar rupture and deformation surfaces, and an empirical formula, suitable for design purposes, is suggested.

Application of the bounds to simple structures indicates that the errors of the bounds for variable loading are greater than those occurring at steady load. However, the increase in error of the upper bound is negligible except when load changes are large and the lower load acts for a large fraction of the total time. Such extreme loading cycles are unlikely to be important in practice. The lower bound is very sensitive to the values of creep index and rupture index and to temperature variations whilst in contrast the upper bound is relatively insensitive. A good, and usually conservative, estimate of the error of the upper bound is given by the error under uniform temperature conditions.

In view of the above comments, design rules based on the upper bound for constant loading

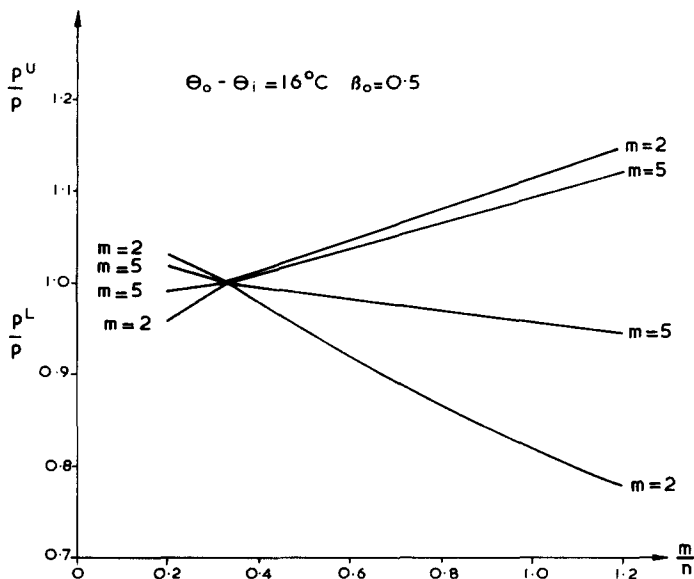


Fig. 8. Tube, effect of m, n on the bounds.

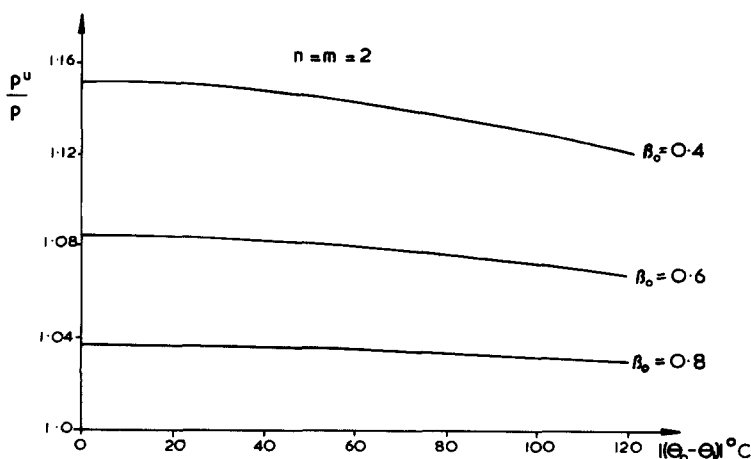


Fig. 9. Tube, effect of temperature difference on the upper bound.

will be useful for variable loading and non-uniform temperature conditions. Goodall *et al.*[5] have proposed that the true load bearing capacity, P and the load bearing capacity, P^u , given by the upper bound can be approximately related by

$$\frac{P^u}{P} = 1 + w(n)(\chi - 1) \tag{6.1}$$

where χ is the ratio of the collapse load to the load to first yield and $w(n)$ is a positive function of the creep index, n . They suggest that a conservative estimate of the true load bearing capacity, for all indices n , may be obtained by setting $w(n) = 0.05$.

For the three structures considered, the ratio (P^u/P) has been plotted against χ on Fig. 11 for steady loading and uniform temperature conditions. A variation in the elastic stress concentration χ is achieved by varying the area and length ratios for the two-bar mechanism and by varying the ratio of internal and external radii for the disc and tube. The creep and rupture indices have been taken equal ($n = m$) and the results plotted are for the highest ratio (P^u/P) in the range $1 \leq n \leq \infty$. Predictions based on these results are, therefore, conservative for the complete range of n . For the two-bar mechanism the maximum ratio occurs at values of n which increase with increasing χ , n being between 2.2 and 3.5 for the results plotted. For the disc, the maxima occur for $n = m \approx 2.8$ and for the tube the maxima are for $n = m \approx 2.4$.

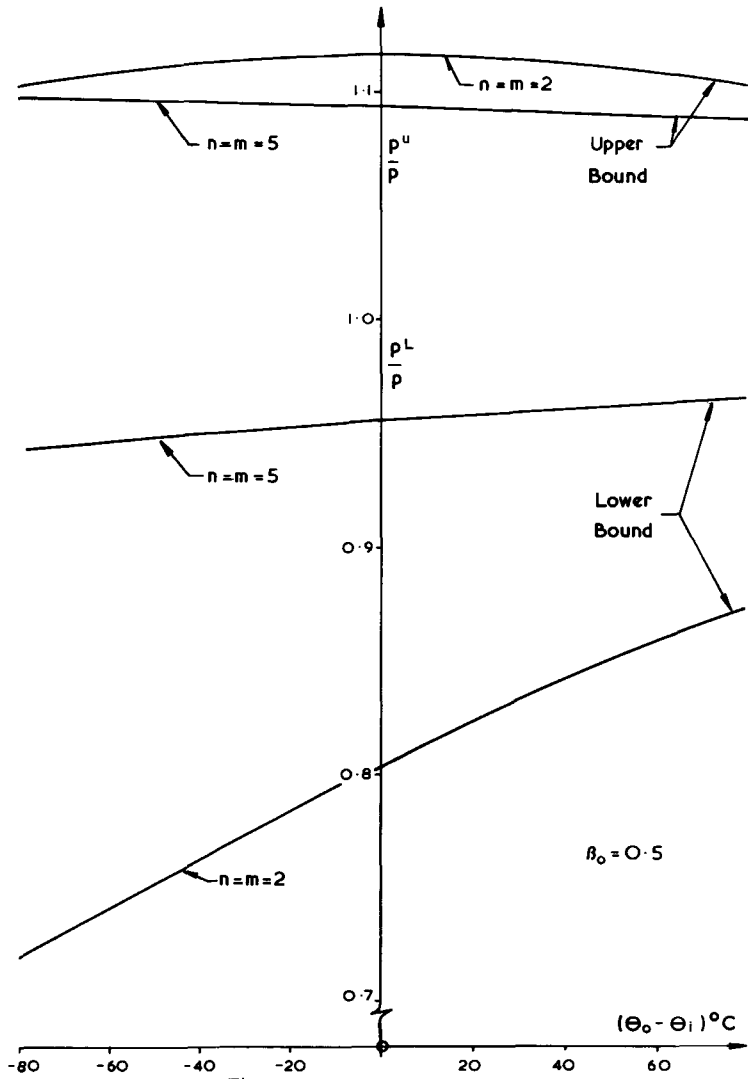


Fig. 10. Tube, upper and lower bounds.

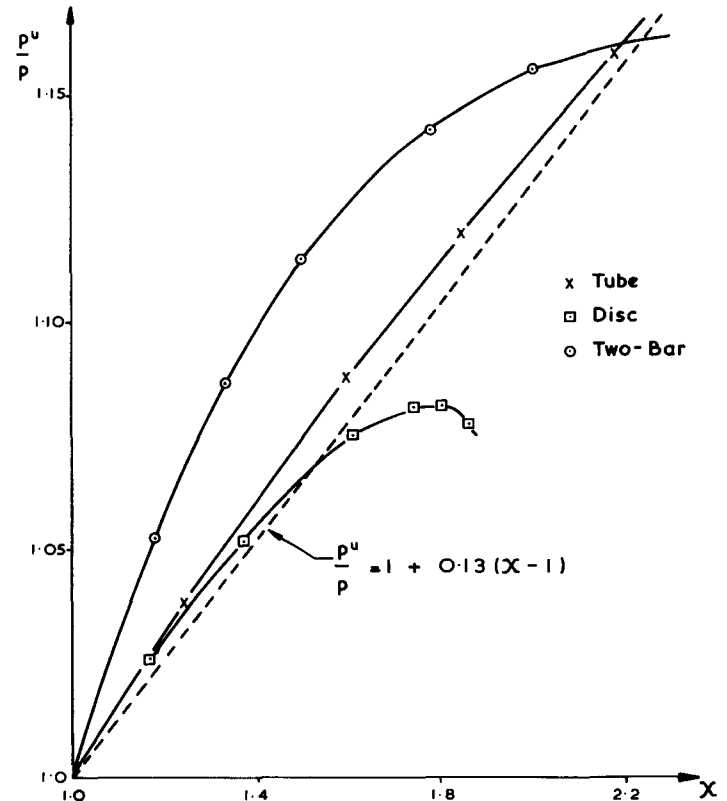


Fig. 11. Variation of the upper bound with χ .

It can be seen from Fig. 11 that a suitable slope is given by $w(n) = 0.13$, although for high values of χ this may be unduly conservative. This slope is greater than the slope $w(n) = 0.05$ suggested by Goodall *et al.*[5], and is in line with results of Goodman[16] obtained for less restrained structures such as torispherical heads. From the present investigation it may be inferred that the simple relationship $P^u/P = 1 + 0.13(\chi - 1)$ should provide a conservative estimate of the load bearing capacity of a fully ductile structure under most loading and temperature conditions.

Acknowledgements—The authors thank Prof. W. S. Hemp, Department of Engineering Science, University of Oxford, for his assistance in this work. This paper is published by permission of the Central Electricity Generating Board.

REFERENCES

1. I. W. Goodall and R. D. H. Cockroft, On bounding the life of structures subjected to steady load and operating within the creep range. *Int. J. Mech. Sci.* **15**, 251 (1973).
2. L. M. Kachanov, Rupture time under creep conditions. *Problems of Continuum Mechanics* (Edited by J. R. M. Radok), p. 202. Society for Industrial and Applied Mathematics, Philadelphia (1961).
3. D. R. Hayhurst, Stress redistribution and rupture due to creep in a uniformly thin plate containing a circular hole. *J. Appl. Mech.* **40**, 224 (1973).
4. D. R. Hayhurst and F. A. Leckie, The effect of creep constitutive and damage relationships upon the rupture time of a solid circular torsion bar. *J. Mech. Phys. Solids* **21**, 431 (1973).
5. I. W. Goodall, R. D. H. Cockroft and E. J. Chubb, An approximate description of the creep rupture of structures. *Int. J. Mech. Sci.* **17**, 351 (1975).
6. J. B. Martin and F. A. Leckie, On time-dependent failure of cracking structures. *J. Mech. Phys. Solids* **20**, 223 (1972).
7. F. A. Leckie and D. R. Hayhurst, Creep rupture of structures. *Proc. Royal Soc. Lond.* **A340**, 323 (1974).
8. E. L. Robinson, Effect of temperature variation on the long time rupture strength of steels. *Trans. Am. Soc. Mech. Engr.* **74**, 777 (1952).
9. R. Hill, New horizons in the mechanics of solids. *J. Mech. Phys. Solids* **5**, 66 (1956).
10. R. Hill, *The Mathematical Theory of Plasticity*. Oxford University Press, Oxford (1950).
11. C. R. Calladine, Time scales for redistribution of stress in creep of structures. *I. Mech. E.* **178**, 3L, 198 (1963).
12. R. A. Ainsworth, Approximate solutions for structures subjected to periodic loading and operating in the creep range. *CEGB Report No. RD/B/N3283* (1975).
13. C. R. Calladine, A rapid method for estimating the greatest stress in a structure subject to creep. *Proc. Roy. Soc. Lond.* **A309**, 363 (1969).
14. Yu. N. Rabotnov, *Creep Problems in Structural Members*. North-Holland, Amsterdam (1969).
15. L. D. Blackburn, Isochronous stress-strain curves for austenitic stainless steels. Presented at the *ASME Winter Annual Meeting*, Nov. 26–30 (1972).
16. A. M. Goodman, The creep design of thin pressure vessel end closures. Presented at the *3rd SMiRT Conference*, London (1975).

APPENDIX 1. PARTICULAR SOLUTION FOR THE RUPTURE OF A THIN DISC

For $n = 1$, the stationary creep solution is the elastic solution

$$\sigma_\theta = \frac{(1 + \alpha^2/\xi^2)}{1 - \alpha^2}, \quad \sigma_r = \frac{1 - \alpha^2/\xi^2}{1 - \alpha^2} \quad (\text{A1.1})$$

where $\xi = r/b$, $\alpha = a/b$ and σ_θ , σ_r are the hoop and radial stress components respectively. The equivalent stress σ_e is then given by

$$\sigma_e^2 = \sigma_r^2 + \sigma_\theta^2 - \sigma_r\sigma_\theta = \frac{1 + 3\alpha^4/\xi^4}{(1 - \alpha^2)^2}. \quad (\text{A1.2})$$

For rupture index $m = 2$, failure will occur at radius ξ at time t for which

$$\int_0^t \frac{1 + 3\alpha^4/\xi^4}{(1 - \alpha^2)^2} d\tau = 1, \quad \text{where } \xi = \alpha(t) \quad (\text{A1.3})$$

and $\alpha = \alpha(\tau)$. Initial failure occurs for $\xi = \alpha_0$ at time t_i given by

$$t_i = \frac{1}{4}(1 - \alpha_0^2)^2 \quad (\text{A1.4})$$

where α_0 is the initial radius ratio. Differentiating (A1.3) twice w.r.t. time gives

$$\alpha(1 - \alpha^2) \frac{d^2\alpha}{dt^2} = 2(1 + \alpha^2) \left(\frac{d\alpha}{dt} \right)^2. \quad (\text{A1.5})$$

(A1.5) can readily be integrated by using the substitution $d\alpha/dt = p$, and using the initial conditions, the final rupture time, t_r , is given by

$$\frac{t_r}{t_i} = 1 + \frac{3\alpha_0}{(1 - \alpha_0^2)^2} \left[\frac{1 - \alpha_0}{\alpha_0} - 2(1 - \alpha_0) + \frac{1 - \alpha_0^3}{3} \right]. \quad (\text{A1.6})$$

Under variable loading, the initial failure time t_i is increased by the factor $[\lambda + (1 - \lambda)\mu^2]^{-1}$ but the final result (A1.6) is unaffected.

APPENDIX 2. UPPER BOUND SOLUTION FOR THIN DISC

The upper bound solution is one for which the equivalent stress σ_e is independent of radius, i.e.

$$\sigma_e^2 = \sigma_r^2 + \sigma_\theta^2 - \sigma_r\sigma_\theta = \text{constant} = A^2, \text{ say} \quad (\text{A2.1})$$

$$\therefore \sigma_\theta = \frac{1}{2}\sigma_r + \frac{1}{2}(4A^2 - 3\sigma_r^2)^{1/2}. \quad (\text{A2.2})$$

The equilibrium condition is

$$r \frac{\partial \sigma_r}{\partial r} = \sigma_\theta - \sigma_r. \quad (\text{A2.3})$$

Combining (A2.2, 3)

$$r \frac{\partial \sigma_r}{\partial r} = -\frac{1}{2}\sigma_r + \frac{1}{2}(4A^2 - 3\sigma_r^2)^{1/2}. \quad (\text{A2.4})$$

Setting $\sigma_r = (2A/\sqrt{3}) \cos \phi$, (A2.4) becomes

$$\frac{1}{2} \int \frac{dr}{r} = \int \frac{\sin \phi \, d\phi}{\cos \phi - \sqrt{3} \sin \phi}. \quad (\text{A2.5})$$

The substitution $\tan \phi = t$ enables (A2.5) to be integrated giving finally

$$\ln(r/a) = -\frac{1}{2} \left[\ln \left| \frac{\sqrt{3}\sigma_r}{2A} - \sqrt{3} \left(1 - \frac{3\sigma_r^2}{4A^2} \right)^{1/2} \right| + \sqrt{3} \cos^{-1} \left(\frac{\sqrt{3}\sigma_r}{2A} \right) \right] + B. \quad (\text{A2.6})$$

The conditions $\sigma_r = 0$, $r = a$ and $\sigma_r = 1$, $r = b$ enable the constants A , B to be evaluated. For $b/a = 4$, $A = 1.183$. The upper bound solution then gives $t_0^* = (1.183)^{-m}$ and

$$t_r \leq \frac{(1.183)^{-m}}{[\lambda + (1 - \lambda)\mu^m]}. \quad (\text{A2.7})$$

APPENDIX 3. CREEP RUPTURE OF A THICK-WALLED CIRCULAR CYLINDER UNDER INTERNAL PRESSURE AND A THROUGH THICKNESS TEMPERATURE GRADIENT

The geometry and loading are shown in Fig. 7. The axial strain rate ϵ_x is assumed zero and from conditions of volume constancy and compatibility this gives

$$\dot{\epsilon}_r = -\dot{\epsilon}_\theta = -Cr^{-2} \quad (\text{A3.1})$$

where $\dot{\epsilon}_r$, $\dot{\epsilon}_\theta$ are the radial and hoop strain rates respectively and C is a constant. The creep rates follow (5.2) so that the plane strain condition requires $S_x = \frac{2}{3}\dot{\epsilon}_x - \frac{1}{3}\dot{\epsilon}_r - \frac{1}{3}\dot{\epsilon}_\theta = 0$ and the equivalent stress then simplifies to

$$\sigma_e = \frac{\sqrt{3}}{2}(\sigma_\theta - \sigma_r). \quad (\text{A3.2})$$

Then from (5.2)

$$\dot{\epsilon}_r = -\dot{\epsilon}_\theta = -\frac{\sqrt{3}}{2}\sigma_e^n g(\theta) \quad (\text{A3.3})$$

where

$$g(\theta) = \exp\{\alpha(\theta - \theta_i)\} \quad (\text{A3.4})$$

and the steady-state temperature distribution is

$$\theta - \theta_i = (\theta_0 - \theta_i) \ln(r/r_i) / \ln(r_0/r_i). \quad (\text{A3.5})$$

Combining (A3.4, 5)

$$g(\theta) = \left(\frac{r}{r_i} \right)^\delta \quad \text{where } \delta = \frac{\alpha(\theta_0 - \theta_i)}{\ln(r_0/r_i)}. \quad (\text{A3.6})$$

The equilibrium condition is

$$r \frac{\partial \sigma_r}{\partial r} = \sigma_\theta - \sigma_r. \quad (\text{A3.7})$$

Combining (A3.1-7) and using the boundary conditions $\sigma_r(r_i) = -p$, $\sigma_r(r_0) = 0$ readily leads to

$$\sigma_e = \frac{\sqrt{3}p}{2} \left\{ \frac{\eta r^{-n}}{r_i^{-n} - r_0^{-n}} \right\} \quad \text{where } \eta = \frac{2 + \delta}{n}. \quad (\text{A3.8})$$

Creep damage will occur and after some time a failure front will propagate either from the inside or the outside. Denote by $\beta(t)$ the ratio of the internal and external radii at time t , $\beta = r_i/r_0$, and by ρ the ratio of radius to external radius $\rho = r/r_0$. If

damage propagates from the outside ρ will be a function of time $\rho(t)$. The stresses are assumed to always have their stationary values given by (A3.8) which in terms of β, ρ is

$$\sigma_c = \frac{\sqrt{3}p}{2} \left\{ \frac{\eta}{\beta^{-n}-1} \right\} \rho^{-n}. \quad (\text{A3.9})$$

The rate of creep damage at any point is

$$\dot{D} = \sigma_c^m g(\theta) = \left(\frac{\sqrt{3}p}{2} \right)^m \beta_0^{-\delta} \left\{ \frac{\eta}{\beta^{-n}-1} \right\}^m \rho^{(\delta-mn)} \left(\frac{r_0(t)}{r} \right)^\delta \quad (\text{A3.10})$$

where β_0 is the initial ratio r_i/r_0 . From (A3.10) there are three possible modes of failure: (a) $m\eta > \delta$, failure occurs at the inside first and propagates to the outside. (b) $m\eta = \delta$, failure occurs at all points simultaneously. (c) $m\eta < \delta$, failure occurs at the outside first and propagates to the inside.

(a) $m\eta > \delta$

The failure front reaches a radius ρ at a time t when the accumulated damage is unity and for which $\beta(t) = \rho$. From (A3.10)

$$\left(\frac{\sqrt{3}p}{2} \right)^m \beta_0^{-\delta} \beta(t)^{(\delta-mn)} \int_0^t \left\{ \frac{\eta}{\beta^{-n}-1} \right\}^m d\tau = 1. \quad (\text{A3.11})$$

Differentiating (A3.11) w.r.t. time, eliminating the integral using (A3.11) and rearranging gives

$$\frac{d\beta}{dt} = \left(\frac{\sqrt{3}p}{2} \right)^m \beta_0^{-\delta} \frac{1}{(m\eta - \delta)} \left\{ \frac{\eta}{1-\beta^n} \right\}^m \beta^{1+\delta}. \quad (\text{A3.12})$$

Initial failure occurs at $\rho = \beta_0$ for time t_i given from (A3.11) by

$$t_i = \left(\frac{\sqrt{3}p}{2} \right)^{-m} \left[\frac{1-\beta_0^n}{\eta} \right]^m. \quad (\text{A3.13})$$

Final failure occurs when the damage reaches the outside $\beta = 1$ at time $t = t_r$. Then from (A3.12)

$$\int_{\beta_0}^1 \left[\frac{1-\beta^n}{\eta} \right]^m \beta^{-(1+\delta)} d\beta = (t_r - t_i) \left(\frac{\sqrt{3}p}{2} \right)^m \beta_0^{-\delta} \frac{1}{(m\eta - \delta)}. \quad (\text{A3.14})$$

Combining (A3.13, 14) gives the pressure p for rupture in time t_r as

$$p = \frac{2}{\sqrt{3}} t_r^{-1/m} \left[\frac{1-\beta_0^n}{\eta} \right] \{1 + (m\eta - \delta)\beta_0^\delta J(\beta_0)\}^{1/m} \quad (\text{A3.15})$$

where

$$J(\beta_0) = \int_{\beta_0}^1 \left[\frac{1-\beta^n}{1-\beta_0^n} \right]^m \beta^{-(1+\delta)} d\beta. \quad (\text{A3.16})$$

(b) $m\eta = \delta$

It immediately follows from (A3.10) that

$$p = \frac{2}{\sqrt{3}} t_r^{-1/m} \left\{ \frac{1-\beta_0^n}{\eta} \right\}. \quad (\text{A3.17})$$

(c) $m\eta < \delta$

Defining $\rho_1 = r/r_i = \rho/\beta$, in like manner to (A3.11), for $\beta(t) = \rho_1^{-1}$

$$\left(\frac{\sqrt{3}p}{2} \right)^m \beta^{(m\eta-\delta)} \int_0^t \beta^{(-m\eta)} \left[\frac{\eta}{\beta^{-n}-1} \right]^m d\tau = 1. \quad (\text{A3.18})$$

The results then follow in identical manner to those for case (a) giving

$$t_i = \left(\frac{\sqrt{3}p}{2} \right)^{-m} \beta_0^\delta \left[\frac{\beta_0^{-n}-1}{\eta} \right]^m \quad (\text{A3.19})$$

$$p = \frac{2}{\sqrt{3}} t_r^{-1/m} \left[\frac{1-\beta_0^n}{\eta} \right] \beta_0^{(\delta/m-n)} \{1 + (\delta - m\eta)\beta_0^{m\eta} J_1(\beta_0)\}^{1/m} \quad (\text{A3.20})$$

where

$$J_1(\beta_0) = \int_{\beta_0}^1 \left[\frac{1-\beta^n}{1-\beta_0^n} \right]^m \beta^{-(1+m\eta)} d\beta \left(\frac{\beta}{\beta_0} \right)^\delta \quad (\text{A3.21})$$

Lower bound

A lower bound on load is given by the load to produce initial failure in time t_r . The lower bound is then obtained by setting

$t_i = t_r$ in (A3.13,19),

$$\begin{aligned} p^L &= \frac{2}{\sqrt{3}} t_r^{-1/m} \left[\frac{1 - \beta_0^n}{\eta} \right], m\eta > \delta \\ p^L &= \frac{2}{\sqrt{3}} t_r^{-1/m} \beta_0^{((\delta/m) - \eta)} \left[\frac{1 - \beta_0^n}{\eta} \right], m\eta < \delta . \end{aligned} \quad (\text{A3.22})$$

For $m\eta = \delta$, $p^L = p$ as given by (A3.17).

Upper bound

The upper bound load bearing capacity is given immediately by replacing η with δ/m in (A3.17)

$$p^u = \frac{2}{\sqrt{3}} t_r^{-1/m} \left[\frac{1 - \beta_0^{\delta/m}}{\delta/m} \right] \quad (\text{A3.23})$$